

# The solution of the positron diffusion trapping model tested for profiling of defects induced by proton implanted in stainless steel

Jerzy Dryzek<sup>1</sup> · Paweł Horodek<sup>1,2</sup>

Received: 23 February 2015 / Accepted: 12 August 2015 / Published online: 21 August 2015  
© Springer-Verlag Berlin Heidelberg 2015

**Abstract** The exact analytical solution of the diffusion trapping model for defect profiling using the variable energy positron beam is reported. The solution is based on the Green's function valid for the case of a discreet step-like vacancy distribution. The solution is applied to the description of experimental data from slow positron beam measurements for samples of stainless steel exposed to high-energy proton multi-implantation. This implantation ensured to obtain an approximate step-like vacancy distribution. The measured annihilation line shape parameter versus positron incident energy is well described by this solution. The determined positron trapping rate, which is proportional to the concentration of vacancies induced during proton implantation, increases linearly with the total dose. The comparison with the commonly used VEPFIT numerical code is also performed. The presented solution can be an alternative to other numerical codes commonly used for evaluation of data from positron beam experiments.

## 1 Introduction

Positron annihilation spectroscopy of slow monoenergetic positrons is commonly used for investigation of defects in a surface adjoining layer of materials [1]. The use of positrons with energy varying in the range 0.1–60 keV allows

us to locate them at the depth from 0.01 nm to several micrometers. It is very convenient for studies of many processes which modify subsurface regions including ion implantation [2]. In this case, defects are generated during slowing down of implanted ions. Due to great mobility vacancies and interstitials annihilate at room temperature, however, a certain fraction of vacancies, divacancies, defect clusters and complexes of defect impurities remain. Their presence can affect the surface and subsurface zone properties of implanted samples.

The basis of the positron annihilation spectroscopy is a great sensitivity of positively charged positrons to the open volume defects, like vacancies along with their clusters, dislocations and their loops. However, one can point out two problems which are relevant for slow positron beam measurements. Only thermalized positrons can be localized at these defects, but before localization, they spend a certain time randomly walking scanning relatively large volume. This diffusion process is well recognized in the slow positron beam technique. Additionally, even monoenergetic positrons are distributed at a wide depth range in a sample during implantation. Thus, the analysis of the obtained data must take both these phenomena into account.

In conventional positron annihilation spectroscopy, the data are analyzed using a trapping model which takes into account only trapping and annihilation rates, assuming the uniform distribution of positrons implanted from a radioactive source. However, the slow positron beam technique requires using the diffusion trapping model (DTM) which is more complex [3]. Usually the numerical approximate algorithms in the VEPFIT [4, 5], ROYPROF [6] and POSTRAP4 [7] codes are applied. Recently, the exact analytical solution of this model based on the Green's function has been obtained [8]. In the paper, we intend to

---

✉ Jerzy Dryzek  
jerzy.dryzek@ifj.edu.pl

<sup>1</sup> Institute of Nuclear Physics Polish Academy of Sciences, ul. Radzikowskiego 152, 31-342 Kraków, Poland

<sup>2</sup> Joint Institute for Nuclear Research, Joliot-Curie 6, Dubna, Moscow region, Russia 141980

test this solution for well annealed samples of stainless steel after high energy, i.e., up to 220-MeV proton multi-implantation. The obtained data from the slow positron beam is also analyzed using the commonly used VEPFIT code.

### 2 The DTM assumptions and solutions

In the model, we assume that positrons are implanted with a certain incident energy in a semi-infinite medium located at positive semi-axis  $0 \leq x \leq \infty$  and the enter surface is placed at the point  $x = 0$ . The distribution of implanted positrons, i.e., those lost their initial energy and start random walk is described by the function  $p(x, E)$ , which also depends on the incident energy  $E$ , Fig. 1. This is the initial condition ( $t = 0$ ) for the following set of time-dependent equations which state DTM:

$$\begin{cases} \frac{\partial n_{\text{bulk}}(x, t)}{\partial t} = D_+ \frac{\partial^2 n_{\text{bulk}}(x, t)}{\partial x^2} - [\lambda_{\text{bulk}} + k(x)]n_{\text{bulk}}(x, t) \\ \frac{dn_{\text{surf}}(t)}{dt} = \alpha n_{\text{bulk}}(x = 0, t) - \lambda_{\text{surf}}n_{\text{surf}}(t) \\ \frac{dn_{\text{def}}(t)}{dt} = \int_0^\infty dx k(x)n_{\text{bulk}}(x, t) - \lambda_{\text{def}}n_{\text{def}}(t) \\ -D_+ \frac{\partial n_{\text{bulk}}(x, t)}{\partial x} \Big|_{x=0} + \alpha n_{\text{bulk}}(x = 0, t) = 0 \end{cases} \quad (1)$$

where  $n_{\text{bulk}}$ ,  $n_{\text{surf}}$  and  $n_{\text{def}}$  represent the number of positrons normalized to the total number of implanted positrons

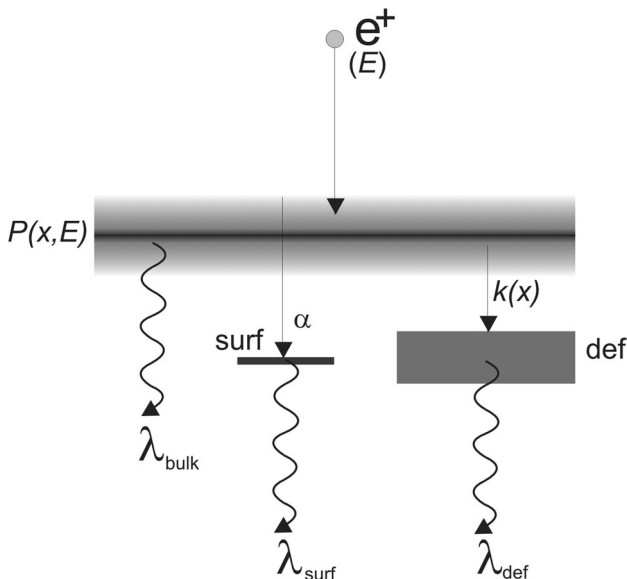


**Fig. 1** Scheme of DTM valid for monoenergetic slow positrons. The gray rectangular at the top represents the region where positrons are implanted and below the region where positrons can be trapped at defects. Annihilation rate from these states and the state at the surface are tagged

which annihilate as free, trapped at the surface and at the defects, respectively. These are the functions of the time  $t$  and depth  $x$ . Only one type of defects which trap positrons is considered; however, their concentration  $C(x)$  varies with the depth and the link with the trapping rate is as follows:  $k(x) = \mu C(x)$ , where  $\mu$  is the specific trapping rate characteristic for a given defect type. The last equation in Eq. (1) represents the radiative boundary condition for the absorption of positrons which can move freely to the surface.  $\alpha$  is the absorption coefficient, and  $D_+$  is the bulk positron diffusion coefficient.  $\lambda_{\text{bulk}}$ ,  $\lambda_{\text{surf}}$ ,  $\lambda_{\text{def}}$  are the annihilation rates for free positrons in bulk, positrons trapped at the surface and defect, respectively.

The analytical solution of Eq. (1) is possible only for a specific function of  $k(x)$ . We argue that the most important from practical point of view is a simple “rectangular step”:

$$k(x) = \begin{cases} k_0, & x \leq x_0 \\ 0, & x > x_0 \end{cases} \quad (2)$$

where  $x_0$  is the total range of the defect profile and  $k_0$  is the trapping rate parameter. This corresponds to the uniform distribution of defects extended from the surface to a certain depth, i.e.,  $x_0$ , no defects are present deeper, where only annihilation from the free state, i.e., bulk takes place.

Combining the Laplace transform and the Green’s function method, one can solve Eq. (1) with such a profile. In Ref. [8], the analytical solution is presented. However, we noticed that the direct application of the relations given in this paper for large value of  $x_0$ , i.e.,  $x_0 \gg \sqrt{D_+/\lambda_{\text{bulk}}}$  or  $k_0$ , can lead to numerical instabilities. The reason is that the number of digits that precede the exponent in the computer codes is typically only the leftmost 15 digits and this is not sufficient. Below, we present the same relations but after algebraic conversions, which allows us to avoid such instabilities:

$$\begin{cases} \tilde{n}_{\text{bulk}}(E) = \int_0^\infty dy \int_0^\infty dx p(x, E) \tilde{G}(y, x) \\ \tilde{n}_{\text{surf}}(E) = \kappa \int_0^\infty dx p(x, E) \tilde{G}(0, x) \\ \tilde{n}_{\text{def}}(E) = q_0 \int_0^{y_0} dy \int_0^\infty dx p(x, E) \tilde{G}(y, x) \end{cases} \quad (3)$$

where  $\kappa = \frac{\alpha}{D_+} L_+$ ,  $L_+ = \sqrt{D_+/\lambda_{\text{bulk}}}$ ,  $q_0 = k_0/\lambda_{\text{bulk}}$ ,  $\tilde{n}_{\text{bulk}}$ ,  $\tilde{n}_{\text{surf}}$  and  $\tilde{n}_{\text{def}}$  represent the Laplace transforms of the time-dependent functions:  $n_{\text{bulk}}$ ,  $n_{\text{surf}}$  and  $n_{\text{def}}$  in the  $s$ -domain for  $s = 0$ . They are the probabilities of annihilation in bulk, at the surface and defects. Similarly, the Green’s function  $\tilde{G}(y, x)$  in the  $s$ -domain for  $s = 0$  is equal to:

$$\tilde{G}(y, x) = \begin{cases} \frac{1}{2} u_2(y) u_1(x), & x \leq y \\ \frac{1}{2} u_2(x) u_1(y), & x \geq y \end{cases} \quad (4)$$

where

$$u_1(x) = \begin{cases} a \exp[(x - y_0)q_1] + b \exp[-(x + y_0)q_1], & x \leq y_0 \\ \exp[(x - y_0)] + \psi \exp[-(x - y_0)], & x > y_0 \end{cases},$$

and

$$u_2(x) = \begin{cases} c \exp[(x - y_0)q_1] + d \exp[-(x - y_0)q_1], & x \leq y_0 \\ \exp(-x + y_0), & x > y_0 \end{cases},$$

and

$$\begin{aligned} \psi &= -\frac{(q_1 - 1)(q_1 + \kappa) + (1 + q_1)(\kappa - q_1) \exp(-2q_1 y_0)}{(q_1 + 1)(q_1 + \kappa) - (1 - q_1)(\kappa - q_1) \exp(-2q_1 y_0)}, \\ a &= \frac{2(q_1 + \kappa)}{(q_1 + 1)(q_1 + \kappa) - (1 - q_1)(\kappa - q_1) \exp(-2q_1 y_0)}, \\ b &= \frac{2(q_1 - \kappa)}{(q_1 + 1)(q_1 + \kappa) - (1 - q_1)(\kappa - q_1) \exp(-2q_1 y_0)}. \\ c &= \frac{1}{2} \left(1 - \frac{1}{q_1}\right), d = \frac{1}{2} \left(1 + \frac{1}{q_1}\right). \end{aligned}$$

Additionally,  $q_1 = \sqrt{1 + q_0}$ ,  $y_0 = x_0/L_+$ . It is easy now to write the suitable relations for the  $S$ -parameter:

$$S(E) = S_{\text{bulk}} \tilde{n}_{\text{bulk}}(E) + S_{\text{surf}} \tilde{n}_{\text{surf}}(E) + S_{\text{def}} \tilde{n}_{\text{def}}(E), \tag{5}$$

where  $S_{\text{bulk}}$  and  $S_{\text{surf}}$  and  $S_{\text{def}}$  represent the corresponding values of the  $S$ -parameter in bulk, at the surface and defects. The mean positron lifetime can be expressed as follows:

$$\bar{\tau}(E) = \tilde{n}_{\text{bulk}}(E)/\lambda_{\text{bulk}} + \tilde{n}_{\text{surf}}(E)/\lambda_{\text{surf}} + \tilde{n}_{\text{def}}(E)/\lambda_{\text{def}}. \tag{6}$$

This equation can be useful for pulsed positron beam which enables us in principle to measure the positron lifetime spectra. The inverse Laplace transform of the set of Eq. (3) could allow us to obtain the positron lifetime spectra for the pulsed beam. However, for analysis of the data from the conventional variable, positron energy beam (VEP) Eq. (5) is sufficient. From Eq. (5), we can obtain relations for the limited conditions, i.e.,  $x_0 = 0$ , it means no defects are presents in the sample [3]:

$$S(E) = S_{\text{bulk}} + \frac{(S_{\text{surf}} - S_{\text{bulk}})}{1 + \kappa^{-1}} \int_0^\infty dx p(x, E) \exp(-x/L_+), \tag{7}$$

and  $x_0 \rightarrow \infty$ , i.e., defects are uniformly distributed in the whole sample:

$$\begin{aligned} S(E) &= \frac{S_{\text{def}} k_0 / \lambda_{\text{bulk}} + S_{\text{bulk}}}{1 + k_0 / \lambda_{\text{bulk}}} + \left( S_{\text{surf}} - \frac{S_{\text{def}} k_0 / \lambda_{\text{bulk}} + S_{\text{bulk}}}{1 + k_0 / \lambda_{\text{bulk}}} \right) \\ &\times \int_0^\infty dx p(x, E) \frac{\exp\left(-\frac{x}{L_+} \sqrt{1 + k_0 / \lambda_{\text{bulk}}}\right)}{1 + \kappa^{-1} \sqrt{1 + k_0 / \lambda_{\text{bulk}}}}. \end{aligned} \tag{8}$$

It should be emphasized that the obtained relations contain the positron implantation profile which should be taken from other calculations, for instance the Monte Carlo simulation of positron trajectories. The Makhovian function is commonly used:

$$p(x, E) = \frac{m x^{m-1}}{x_0^m} \exp\left[-\left(\frac{x}{x_0}\right)^m\right], \tag{9}$$

where

$$x_0 = \frac{A_{1/2}}{\rho(\ln 2)^{1/m}} E^n,$$

$\rho$  represents the density of the implanted medium and the values of other parameters, i.e.,  $n$ ,  $m$  and  $A_{1/2}$ , one can find in Ref. [9]. However, the other relations, for instance, proposed by Ghosh et al. [10] or the Gaussian derivative,  $m = 2$ , can be used as well. (In the calculations of set of Eq. (3)  $x_0$  in Eq. (9) should be replaced by  $x_0/L_+$ .)

The VEP data contain certain amount of the so-called epithermal positrons whose energy is much higher than thermal energy and they can annihilate close to or on the enter surface. In the literature, authors propose to describe them by the scattering length  $L_{\text{epith}}$  parameter, whose value is about few nanometers [1, 11]. Then the measured profile of the  $S$ -parameter can be expressed as follows:

$$S'(E) = S(E)[1 - J(E)] + S_{\text{epith}} J(E), \tag{10}$$

where  $J(E) = \int_0^\infty dx p(x, E) \exp(-x/L_{\text{epith}})$  and  $S_{\text{epith}}$  is the  $S$ -parameter value corresponding to the epithermal positrons trapped at the surface. We argue that the relation presented above can describe the dependency of the annihilation line shape  $S$ -parameter on positron incident energy obtained in the VEP experiments.

### 3 The experimental details

In our studies, we used stainless steel, i.e., 304 AISI containing 0.04 % C, 1 % Si, 2.0 % Mn, 17.0 % Cr and 9 % Ni. The samples were prepared in the form of disks 15 mm in diameter and 5 mm thick. Surfaces were sequentially polished, first using silicon carbide waterproof abrasive paper and next polishing machine Tecmet 2000-MP21 V on the polishing cloth. Then four specimens were annealed in a furnace for 2 h at 800 °C in vacuum  $6 \times 10^{-6}$  mbar and cooled slowly to the room temperature. Such a treatment, according to our former studies, is sufficient to obtain samples with only residual defects [12].

In order to obtain the “rectangular” defect depth profile, at room temperature, the proton implantation was performed using the apparatus (UNMIAS 79) available at Institute of Physics Maria Curie-Skłodowska University in Lublin in Poland. The current was equal to 0.2  $\mu\text{A}$ , and the

**Table 1** Energies and doses applied during proton multi-implantation into three stainless steel samples

Energy (keV)	Dose (ion/cm <sup>2</sup> )		
	Sample 1 (S1)	Sample 2 (S2)	Sample 3 (S3)
220	$3.0 \times 10^{14}$	$1.0 \times 10^{15}$	$3.0 \times 10^{15}$
195	$1.5 \times 10^{14}$	$0.5 \times 10^{15}$	$1.5 \times 10^{15}$
170	$1.2 \times 10^{14}$	$0.4 \times 10^{15}$	$1.2 \times 10^{15}$
150	$1.1 \times 10^{14}$	$0.4 \times 10^{15}$	$1.1 \times 10^{15}$
135	$0.6 \times 10^{14}$	$0.2 \times 10^{15}$	$0.6 \times 10^{15}$
115	$0.8 \times 10^{14}$	$0.3 \times 10^{15}$	$0.8 \times 10^{15}$
95	$1.3 \times 10^{14}$	$0.4 \times 10^{15}$	$1.3 \times 10^{15}$
Total	$9.5 \times 10^{14}$	$3.2 \times 10^{15}$	$9.5 \times 10^{15}$

spot diameter was 3.5 cm. Protons were injected sequentially with different energies and fluences (see Table 1) starting from the biggest ones. The irradiation time depended on the applied dose, and it was less than 15 min. The vacuum conditions were on the level of  $10^{-6}$  Pa.

The VEP measurements were taken at Low Energy Particle Toroidal Accumulator (LEPTA) facility at Joint Institute for Nuclear Research (JINR) in Dubna [13, 14]. The frozen Ne was used as the moderator for <sup>22</sup>Na positrons. The positron flux with intensity of about  $3 \times 10^5$  e<sup>+</sup>/s and energy range between 50 eV and 35 keV was obtained. Spectra of annihilation line were collected with HpGe detector with Gaussian resolution function of FWHM = 1.20 keV. The line was characterized by the *S*-parameter defined as the ratio of area under the central part of 511 keV line to the total area below this line. Both parameters were calculated using SP-1 code [15].

In our calculations, we adopt the Makhovian function (9) for the description of the positron implantation profile. The parameters are taken from Ref. [9] as for Fe, i.e.,  $m = 1.766$ ,  $n = 1.692$  and  $x_0$  (nm) =  $3.7373 \times E^{1.692}$ , and  $E$  is the incident positron energy in keV.

## 4 Results and discussion

Varying the energy of implanted protons allows us to generate almost constant distribution vacancies at a certain depth only, and thus, this corresponds to the assumption of DTM presented above. To confirm this, we performed simulations of the vacancy distribution employing Monte Carlo simulations in commonly used SRIM/TRIM code, [16, 17]. In Fig. 2, we depicted the obtained results of the generated vacancy concentration versus depth from the enter surface. For all samples, this concentration is almost constant in the range from 400 to 980 nm. The concentration increases with the increase in the applied total dose. Close to the surface, the decrease is noticed; however, it

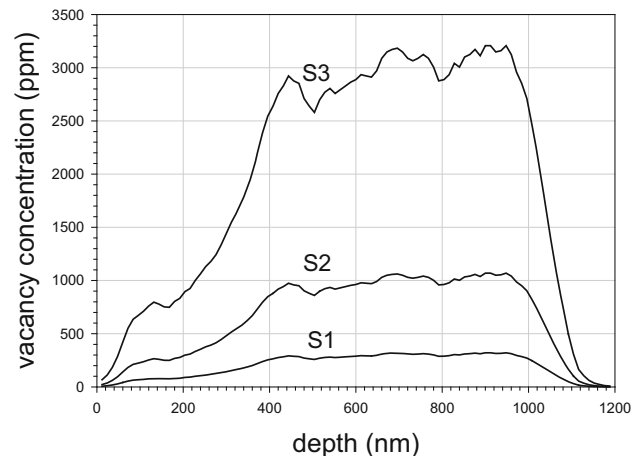


**Fig. 2** Monte Carlo simulations of the vacancy depth distribution induced by energetic proton multi-implantation in the stainless steel samples generated with the use of the SRIM/TRIM code. The energies and doses of the implanted protons are given in Table 1. The almost rectangular shape of the profile is obtained for all samples

will be neglected in our consideration. It should be point out that in the literature, authors apply ion implantation with only single energy and then assume also rectangular distribution of defects for analyzing their VEP data using the VEPFIT code (see, for instance, Ref. [18]). We argue that our samples despite of unavoidable irregularities seen in Fig. 2 fulfill the assumption much better.

The measured dependencies of the *S*-parameter versus the positron incident energy for all studied stainless steel samples are depicted in Fig. 3. We can enumerate the characteristic features. For the reference, (Ref) well annealed and non-implanted sample, closed circles in Fig. 3, the decrease in the *S*-parameter is well recognized for the whole energy range. For the implanted samples: S1, S2 and S3, the decrease is stopped at the energy of about 5 keV and saturation appears up to energy of about 20 keV. The value of the *S*-parameter in this energy range increases with the increase in the total dose, see Table 1. Above 20 keV the decrease in the *S*-parameter is observed again. The value of the *S*-parameter at the surface, i.e., for minimal positron energies is very similar for all the samples. Also for the higher incident energy, the *S*-parameter values tend to the value for the reference sample. Thus, the changes observed are induced by the presence of defects generated during implantation. Similar dependencies were observed by many authors who implanted other ions into samples, and the results are presented, for instance, in Ref. [1]

For the reference sample, the dependency can be well described by Eq. (10) including (7). The best fit of this relation is obtained for the following values of the adjustable parameters:  $L_+ = 73.3 \pm 1.7$  nm,  $S_{\text{bulk}} = 0.486(1)$ ,  $S_{\text{surf}} = 0.561(1)$  and  $\kappa = 3.9(6)$ , and the solid line in Fig. 3 represents this fit. The parameters which describe epithermal

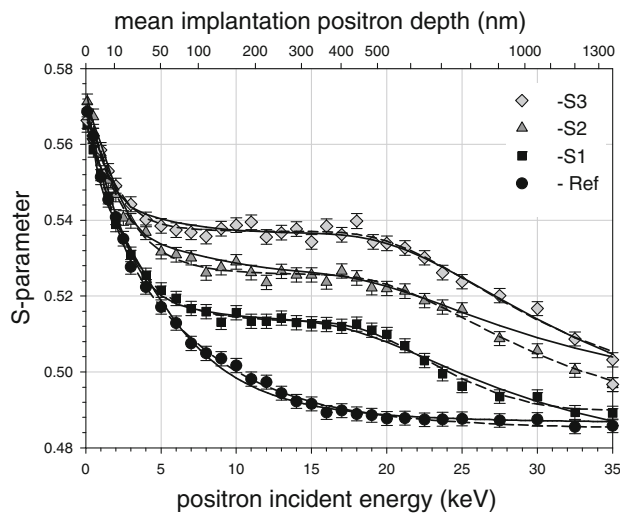


**Fig. 3** Dependency of the  $S$ -parameter values on the incident positron energy for all measured samples. The *solid lines* represent the best fits of DTM. For the reference sample, Ref, Eq. (10) with (7) is used, and for the samples S1, S2 and S3, Eqs. (10) and (5) with (3) are applied. The *dashed lines* represent the results obtained using the VEPFIT codes. At *top axis*, the average positron implantation depth is calculated according to the equation:  $\bar{x}(\text{nm}) = 3.32 \times E^{1.692}$ ,  $E$  is the incident positron energy in keV

positron are equal to  $S_{\text{epith}} = 0.572(1)$  and  $L_{\text{epith}} = 1.5$  nm. The latter is fixed in our calculations. The diffusion length  $L_+$  is the most important parameter, which determines the capability of the stainless steel host to transport thermalized positrons. Its value corresponds to the value for other metals reported in Ref. [1]. The diffusion length determined for pure defect free iron is about  $142 \pm 2$  nm, and it is higher than for stainless steel [19]. It is well understood because stainless steel contains also alloying elements and impurities. They can scatter positrons and affect the diffusion length value. The values of obtained parameters correspond well with those obtained using the VEPFIT code. For this case,  $L_+ = 73.6 \pm 2.0$  nm,  $S_{\text{bulk}} = 0.486(2)$ ,  $S_{\text{surf}} = 0.548(5)$ ,  $S_{\text{epith}} = 0.572(1)$  and  $\kappa = 26(8)$ . It can be noticed the slightly different value for  $S_{\text{surf}}$ . However, this parameter can interfere with the  $S_{\text{epith}}$  because either  $J(E)$  and  $\tilde{n}_{\text{surf}}(E)$  are the monotonically decaying functions with increasing incident energy, Fig. 4. Also the  $\kappa$  parameter describing the surface absorption capability differs in both cases. We noticed that this parameter hardly affects the fitted dependencies, and then, for instance, in ROYPROF code, its value is assumed to be infinity [6]. The  $S_{\text{bulk}}$  values determined by both methods coincide perfectly. This is due to the fact that  $\tilde{n}_{\text{bulk}}(E)$  is an increasing function with saturation at higher incident energy and there is no overlapping with  $\tilde{n}_{\text{surf}}(E)$  and  $J(E)$  dependencies. The dependency obtained with the VEPFIT code is depicted as dashed line in Fig. 3. The overlapping with that obtained from Eq. (10) including (7) is clearly visible.

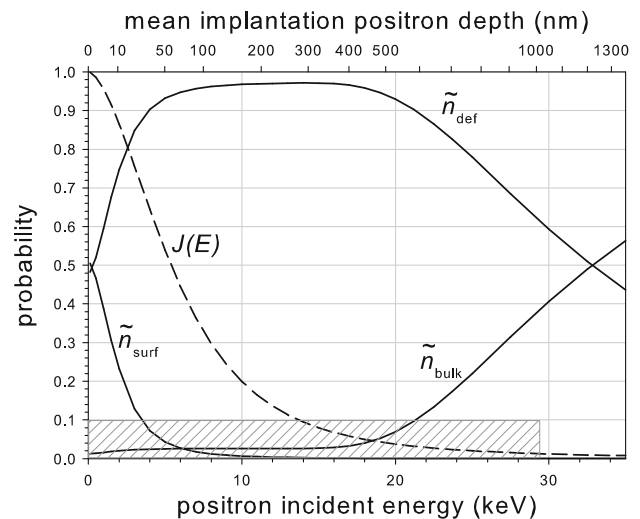


**Fig. 4** Calculated probability of positron annihilation in bulk  $\tilde{n}_{\text{bulk}}$ , at the surface  $\tilde{n}_{\text{surf}}$  and trapped at the defects  $\tilde{n}_{\text{def}}$  as the function of the positron incident energy. The parameters for the calculation are assumed  $k_0 = 0.35$  ps $^{-1}$ ,  $x_0 = 1080$  nm,  $L_+ = 73$  nm,  $\alpha = 4.4$  nm/ps,  $\lambda_{\text{bulk}} = 1/106$  ps $^{-1}$ . The *hatched rectangular region* shows the scheme of the assumed vacancy depth distribution

For the description of implanted samples, Eq. (10) including (5) is used. The solid lines in Fig. 3 represent the obtained fits. The agreement with the experiment points is well visible with the regression coefficient about 0.98. The most important parameters are related to the defect profile, i.e., the trapping rate  $k_0$  and vacancy distribution range  $x_0$ . For sample S1,  $k_0 = 0.04$  ps $^{-1}$  and  $x_0 = 840$  nm. Other parameters are gathered in Table 2. For comparison, the parameters obtained from VEPFIT code are also presented. Model 5 of VEPFIT with two layers is used. The first layer corresponds to the rectangular distribution of defects and the second one to the bulk region. The good agreement was achieved; however, a discrepancy is noticed for  $S_{\text{surf}}$  parameter. The value obtained from VEPFIT is about twice higher than obtained from calculation using the above relations. This can be explained by two reasons. VEPFIT code assumes the approximated, polynomial form for the positron implantation profile. In the region adjoining the surface, the profile varies rapidly, which can cause that polynomial is a crude approximation. In our samples, the defect distribution in all samples decreases close to the surface according to the SRIM/TRIM code, Fig. 2, and this is not taken into account in our model. It can cause the discrepancy in the determination of  $S_{\text{surf}}$  parameter. One should point out that in Ref. [18], the author compared the fitted parameters obtained with three codes: ROYPROF, VEPFIT and POSTRAP4, see Table 1. Also in this case, the small differences between values of  $S_{\text{surf}}$  occurred, whereas the values of  $S_{\text{bulk}}$  and  $S_{\text{def}}$  are equal within the accuracy. Likewise, in this case, the dependencies obtained

**Table 2** Values of the  $S$ -parameters obtained from the fit of Eq. (10) with (7) for reference sample (Ref) and Eqs. (10) and (5) with (3) for the samples S1, S2 and S3 and corresponding parameters obtained from the VEPFIT code (in italics)

	Ref	S <sub>1</sub>	S <sub>2</sub>	S <sub>3</sub>
$S_{\text{bulk}}$	0.486(1) <i>0.486(1)</i>	0.476(2) <i>0.477(1)</i>	0.491(2) <i>0.479(1)</i>	0.479(2) <i>0.481(1)</i>
$S_{\text{surf}}$	0.561(1) <i>0.548(1)</i>	0.363(1) <i>0.559(1)</i>	0.318(20) <i>0.567(1)</i>	0.315(3) <i>0.589(2)</i>
$S_{\text{def}}$		0.521(1) <i>0.513(1)</i>	0.527(1) <i>0.526(1)</i>	0.537(1) <i>0.537(1)</i>
$S_{\text{epith}}$	0.572(1) <i>0.572(1)</i>	0.562(1) <i>0.565(1)</i>	0.568(6) <i>0.573(1)</i>	0.567(1) <i>0.566(1)</i>
$k_0$ (ps <sup>-1</sup> )		0.04 <i>0.08</i>	0.10 <i>0.13</i>	0.35 <i>0.35</i>
$x_0$ (nm)		840(10) <i>804(20)</i>	940(30) <i>1017(30)</i>	1080(17) <i>1060(10)</i>

The trapping rate parameter  $k_0$  is calculated according the relation:  $k_0 = \lambda_{\text{bulk}}[(L_{\text{bulk}}/L_+)^2 - 1]$ , where  $L_{\text{bulk}} = 73.3 \pm 1.7$  nm and  $L_+$  is the diffusion length determined from VEPFIT code and  $\lambda_{\text{bulk}} = 1/106$  ps<sup>-1</sup>

with the VEPFIT code are depicted as dashed lines in Fig. 3 and they overlap these obtained from Eq. (10) including (3).

In Fig. 4, we drew the probabilities of annihilation in bulk, at the surface, at defect and  $J(E)$  for illustration of Eq. (3), with parameters as for S3. With the increase in the incident energy, the probability of annihilation at the surface decreases, and the probability of annihilation in bulk increases. This is well understood because only positrons implanted close to the surface have a chance to come back to the surface and annihilate there. The probability of annihilation in defect exhibits different dependencies, it saturates at the energy between 5 and 20 keV, and above it decreases. The decrease is also close to the surface, because the surface being the positron trap as well is a competition for trapping at defects. This is well understood taking into account the fact that positrons diffuse before annihilation. Note  $\tilde{n}_{\text{bulk}} + \tilde{n}_{\text{surf}} + \tilde{n}_{\text{def}} = 1$ , for each energies. One can emphasize that despite the fact that vacancy distribution is rectangular, the dependencies of probabilities are smeared, and non-“rectangular shape” of dependencies is noticeable. This is well understood, because in the experiment, we cannot stop positrons at a certain distance and then prevent diffusion, and in Fig. 4, it is clearly visible. Both processes significantly affect the experimental response of VEP results. We can also notice that distribution of epithermal positrons, i.e.,  $J(E)$  correlates with  $\tilde{n}_{\text{surf}}(E)$  function close to the surface and this can interfere while determination of the  $S_{\text{surf}}$  parameter value.

The depths of the defect distribution obtained from the fits and presented as solid lines in Fig. 3 are as follows: for S1,  $x_0 = 840(10)$  nm, S2,  $x_0 = 940(30)$  nm and S3,  $x_0 = 1080(17)$  nm, they are also close to those obtained from the VEPFIT code, Table 2. For S2 and S3,  $x_0$  value corresponds well with the cut of the distribution seen in

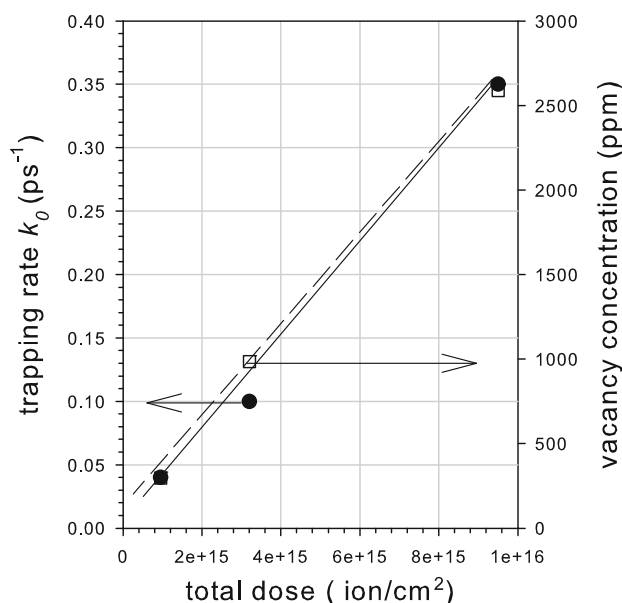


**Fig. 5** Dependence of the trapping rate,  $k_0$ , obtained from the assumed DTM as the function of total dose of implanted protons. On the right vertical axis, the simulated average vacancy concentration in the range 400–980 nm is taken from Fig. 2. The solid and dashed lines represent the linear least square fits to the points

Fig. 2. However, for S1, it is underestimated by about 20 %. It can be related to the dose effect, which is not taken into account in SRIM/TRIM code. The most important is the trapping rate parameter  $k_0$ . Its values are depicted in Fig. 5 as the function of the dose. The linear increase is evident. In this figure, the value of the average vacancy concentration taken from Fig. 2 is also added. Such a dependency was obtained by many authors, for instance in Si implanted with different ions [20]. As it was expected, both dependencies almost overlap themselves.

One can attempt to obtain the value of the specific trapping rate  $\mu$  from these data. It links the measured trapping rate and vacancy concentration. In this case, its average value is equal to  $\mu = 115 \text{ ps}^{-1}$ , or  $170 \text{ ps}^{-1}$  determined from VEPFIT results. For vacancies in  $\alpha$ -Fe, this value was estimated to about  $10^3 \text{ ps}^{-1}$  [21]. The agreement is good taking into account the fact that the vacancies were generated during proton implantation annihilate at room temperature and only certain part of them survive.

One should also point out that the obtained solutions Eq. (3) can be applied to the description of data for semiconductors, where the electric field affects the positron diffusion close to the surface. This requires to subtract the drift term in the first equation in Eq. (1), i.e.,  $v \frac{\partial n_{\text{bulk}}(x,t)}{\partial x}$ , where  $v$  is the drift velocity. As it was shown in Ref. [3], it requires to replace  $\lambda_{\text{bulk}}$  with  $\lambda_{\text{bulk}} + \frac{v^2}{4D_+}$  and  $\alpha$  with  $\alpha + v/2$  in Eq. (3) to have the solution for such a case.

## 5 Conclusions

The improved relations of exact, analytical solution of DTM for VEP experiment have been tested. The test was performed for the stainless steel samples implanted with energetic protons in such a way that almost rectangular distribution of vacancies was achieved. This was confirmed using the SRIM/TRIM codes. The positron annihilation Doppler broadening parameter adjusted with the VEPFIT numerical code and the relations are consistent. However, the discrepancy for parameter corresponding to the surface  $S_{\text{surf}}$  is noticed, and this can arise from the fact that the positron implantation profile close to the surface is taken into account in more detail than in the numerical code. The improved relations based on the Green's function method do not display numerical instabilities and can describe the VEP data with satisfactory result.

**Acknowledgments** The authors express their gratitude to M. Kulik, M. Turek, K. Pysznik and A. Drozdziel for their technical help assistance at ion implantation.

## References

1. P.J. Schultz, K.G. Lynn, *Rev. Mod. Phys.* **60**, 701 (1988)
2. R. Krause-Rehberg, H.S. Leipner, *Positron Annihilation in Semiconductors, Defect Studies* (Springer, Berlin, Heidelberg, New York, 2000)
3. J. Dryzek, *Nucl. Instrum. Methods Phys. Res. B* **196**, 186 (2002)
4. G.C. Aers, K.O. Jensen, A.B. Walker, in *Slow Positron Beam Techniques for Solids and Surfaces*, vol. 303, ed. by E. Ottewitte, A.H. Weiss, AIP Conference Proceedings (AIP Press, New York, 1994), p. 13
5. A. van Veen, H. Schut, J. de Vries, R.A. Hakvoort, W.R. Ijmpa, in *Positron beam for solids and surfaces*, vol. 218, ed. by J. Schultz, G.R. Massoumi, P.J. Simpson, AIP Conference Proceedings (AIP Press, New York, 1990), p. 171
6. A.S. Saleh, J.W. Taylor, P.C. Rice-Evans, *Appl. Surf. Sci.* **149**, 87 (1990)
7. G.C. Ares, in *Positron Beams for Solids and Surfaces*, ed. by P.J. Schultz, G.R. Massoumi, P. Simpson (AIP, New York, 1991)
8. V.A. Stephanovich, J. Dryzek, *Phys. Lett. A* **377**, 3038 (2013)
9. J. Dryzek, P. Horodek, *Nucl. Instrum. Methods Phys. Res. B* **266**, 4000 (2008)
10. V.J. Ghosh, D.O. Welch, K.G. Lynn, in *Positron Beam Techniques for Solids and Surfaces*, vol. 303, ed. by E. Ottewitte, A.H. Weiss, Jackson Hole, Wyoming, AIP Conference Proceedings, New York (1994), p. 37
11. D.T. Britton, P.C. Rice-Evans, J.H. Evans, *Philos. Mag. Lett.* **57**, 165 (1988)
12. J. Dryzek, P. Horodek, M. Wróbel, *Wear* **294–295**, 264 (2012)
13. A.A. Sidorin, I. Meshkov, E. Ahmanova, M. Eseev, A. Kobets, V. Lokhmatov, V. Pavlov, A. Rudakov, S. Yakovenko, The LEPTA facility for fundamental studies of positronium physics and positron spectroscopy. *Mater. Sci. Forum* **733**, 291 (2013)
14. A.A. Sidorin, I. Meshkov, E. Ahmanova, M. Eseev, A. Kobets, V. Lokhmatov, V. Pavlov, A. Rudakov, S. Yakovenko, Positron annihilation spectroscopy at LEPTA facility. *Mater. Sci. Forum* **733**, 322 (2013)
15. J. Dryzek, [http://www.ifj.edu.pl/~mdryzek/page\\_r18.html](http://www.ifj.edu.pl/~mdryzek/page_r18.html). Accessed 1 Aug 2013
16. J.F. Ziegler, M.D. Ziegler, J.P. Biersack, *Nucl. Instrum. Methods Phys. Res. B* **268**, 1818 (2010)
17. J.F. Ziegler, J.P. Biersack, [http://www.srim.org/SRIM/SRIMIN\\_TRO.htm](http://www.srim.org/SRIM/SRIMIN_TRO.htm). Accessed 10 April 2012
18. A.S. Saleh, *J. Theor. Appl. Phys.* **7**, 39 (2013)
19. F. Lukáč, J. Čížek, I. Procházka, Y. Jirásková, D. Janičkovič, W. Anwand, G. Brauer, *J. Phys: Conf. Ser.* **443**, 012025 (2013)
20. A.P. Knights, F. Malik, P.G. Coleman, *Appl. Phys. Lett.* **75**, 466 (1999)
21. H.-E. Schaefer, *Phys. Status Solidi A* **102**, 47 (1987)